SDSS'Rio 2010 STABILITY AND DUCTILITY OF STEEL STRUCTURES
E. Batista, P. Vellasco, L. de Lima (Eds.)
Rio de Janeiro, Brazil, September 8 - 10, 2010

LOCAL POST-BUCKLING BEHAVIOUR OF ELLIPTICAL TUBES

Nuno Silvestre* and Leroy Gardner**

* Department of Civil Engineering, IST-ICIST, Technical University of Lisbon, Portugal
nuno.silvestre@civil.ist.utl.pt

** Department of Civil and Environmental Engineering, Imperial College London, United Kingdom
leroy.gardner@imperial.ac.uk

Keywords: Buckling, Elliptical Hollow Sections, Oval Hollow Sections, Post-buckling, Steel Structures.

Abstract. *The local post-buckling behaviour of elliptical hollow section (EHS) tubes under compression is analysed in this paper. It is found that EHS tubes with low to moderate aspect ratios can support loads up to their limit loads but are imperfection sensitive (shell-type behaviour), while EHS tubes with moderate to high aspect ratios can carry loads higher than their limits loads (plate-type behaviour) and are imperfection insensitive. For increasing EHS aspect ratio, it is found that the compressive stresses accumulate near the zones of minimum radius of curvature while the zones of maximum radius of curvature experience a relatively low compressive stress level. Thus, it is likely to apply the effective width concept to EHS tubes with moderate to high aspect ratio.*

1 INTRODUCTION

EHS steel tubes are now available as hot-rolled structural products [1,2] and represent an interesting solution for many visible applications in steel construction, particularly for glass facades. These shapes are included in the new edition of EN 10210 [3] and are available in a standard range of dimensions. In response to the emergence and commercial availability of EHS tubes, several recent investigations on their buckling behaviour and strength have been published. Gardner and Chan [4] and Chan and Gardner [5,6] assessed the non-linear behaviour of hot-rolled EHS tubes by means of experimental and numerical analyses and proposed structural design rules. They found that the slenderness limits for pure compression set out in EC3 for circular hollow section (CHS) classification can be safely adopted for EHS, based on the equivalent diameter of the point of the EHS with maximum radius. Zhu and Wilkinson [7] also performed shell finite element analyses to evaluate the buckling and post-buckling behaviour of EHS in compression. Silvestre [8] developed a formulation of Generalised Beam Theory (GBT) to analyse the elastic buckling behaviour of members with non-circular hollow sections (NCHS) and applied it to study the behaviour of EHS shells and tubes under compression, particularly the variation of the critical buckling stress with the member length and cross-section geometry. Ruiz-Teran and Gardner [9] have also examined the buckling response of EHS tubes in compression and proposed analytical formulae to accurately predict the critical stress. Thus, the main objective of this paper is to unveil the mechanics of the elastic local post-buckling behaviour of EHS tubes and to explain in a detailed fashion the transition between the shell-type (imperfection sensitive) behaviour of EHS tubes with low eccentricity and the plate-type (imperfection insensitive) behaviour of EHS tubes with high eccentricity.

2 PARAMETRIC STUDY

An in-depth study on the influence of the EHS aspect ratio on the variation and nature of the post-buckling equilibrium path, ensuing stress distributions and imperfection sensitivity is presented. A reference EHS stub column with length L = 300 mm, thickness t = 4 mm and fully fixed supports is

considered. The EHS geometry is characterised by the major axis width 2a and minor axis width 2b, which are considered here as the dimensions of the EHS mid-line (i.e., 2a + t and 2b + t are the outer dimensions). Based on a commercially available [1,2] reference geometry (2a = 150 mm, 2b = 75 mm, a/b = 2.0), five further EHS configurations were generated and studied. These were obtained by (i) keeping the cross-section perimeter unaltered (P = 363 mm) and (ii) varying the aspect ratio a/b from 1.10 to 5.0. The six EHS geometries considered in this paper are represented in figure 1 and are characterised by an equal cross-section area A=1450 mm^2 and thus an equal amount of steel in each column.

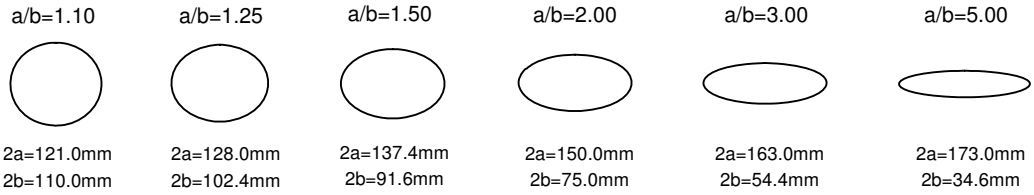

Figure 1: Selected EHS geometries and corresponding aspect ratio a/b.

3 SHELL FINITE ELEMENT MODEL

The local post-buckling behaviour of EHS tubes under compression is investigated numerically using the finite element code ABAQUS [10]. In order to analyse the local behaviour of a given thin-walled member, one must adopt a two-dimensional model to discretise its mid-surface, a task that can be adequately performed by means of 4-node isoparametric shell elements with reduced integration (S4R elements in the ABAQUS nomenclature). In the case of the EHS tubes dealt with in this work, discretisation of the cross-section into 36 finite elements was found to be sufficient − this corresponds roughly to adopting 10 mm wide elements. A mesh size of 5 mm in the length direction was used, leading to a total of 2160 elements and 2196 nodes. In order to ensure adequate modelling of the fixed end support conditions, rigid plates were attached to the stub column end sections, thus preventing all local and global displacements and rotations, including (i) rigid-body motions (with the exception of the axial translation of the loaded end section), (ii) warping and (iii) in-plane deformation. These rigid end plates were modelled by means of 3-node R3D3 finite elements (again ABAQUS nomenclature). The compressive load was applied through the centroid of the axially free end section and, in order to obtain the load versus axial shortening equilibrium path, the corresponding axial displacement was assessed by using an ABAQUS command termed "MONITOR".

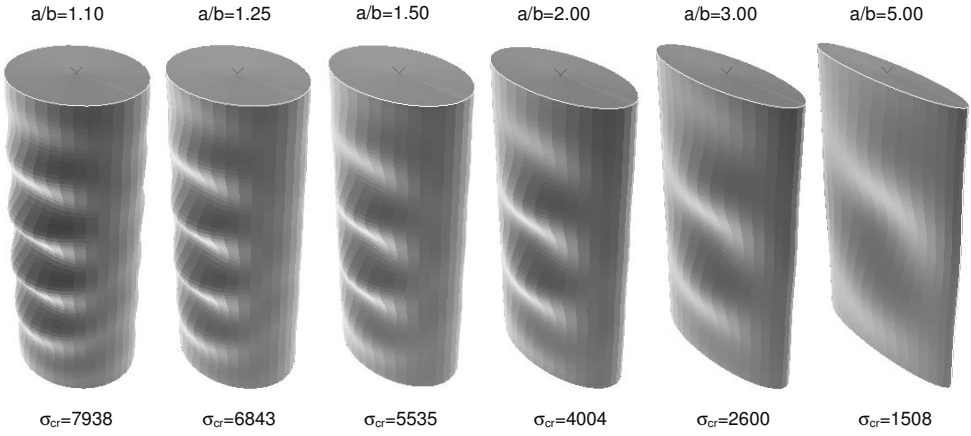

Figure 2: Critical buckling modes and corresponding critical stresses σ_{cr} (in N/mm^2)

The material behaviour of the steel tube was assumed to be homogeneous, isotropic and linear elastic, which is fully characterised by the values of Young's modulus (E = 210000 N/mm^2) and Poisson's ratio (ν = 0.3). Initial geometrical imperfections were included in the models in the form of the most relevant (critical) local buckling mode shapes, incorporated into the tube initial geometry by means the initial conditions ABAQUS command. Therefore, preliminary buckling (eigenvalue) analyses were carried out for all the six columns in order to obtain the local buckling stress values and the corresponding buckling mode configurations, which are depicted in figure 2. For the initial studies, a small imperfection amplitude equal to 0.1 mm (2.5% of EHS thickness) was adopted, while imperfection sensitivity is investigated further in Section 6 of this paper. No residual stresses were incorporated into the numerical analyses, since they were deemed to be of very low magnitude in hot-finished elliptical tubes [5].

4 NON-LINEAR EQUILIBRIUM PATHS

Before introducing the study on the influence of the EHS aspect ratio on the variation and nature of the post-buckling equilibrium path and ensuing stress distributions, the variation of the local critical buckling stress with the EHS aspect ratio a/b is first assessed. For the six different aspect ratios considered herein, the values of the critical buckling stress σ_{cr} (N/mm^2) are given in table 1. As expected, it may be seen that the critical stress decreases with increasing aspect ratio, almost inversely. Having examined the elastic critical buckling behaviour of EHS, subsequent studies of the elastic post-buckling behaviour were then performed. The non-linear equilibrium paths (applied stress σ versus axial shortening u) obtained from the post-buckling analyses are plotted in figure 3(a)). The same results are presented in a normalised format – critical stress ratio σ/σ_{cr} versus critical strain ratio $\varepsilon/\varepsilon_{cr}$ – in figure 4.

Table 1: Critical stresses and limit stresses obtained from FE models

a/b	σ_{cr} (N/mm^2)	σ_{lim} (N/mm^2)	σ_{lim}/σ_{cr}
1.10	7938	6810	0.86
1.25	6843	5988	0.88
1.50	5535	4600	0.83
2.00	4004	3555	0.89
3.00	2600	2130	0.82
5.00	1508	1202	0.80

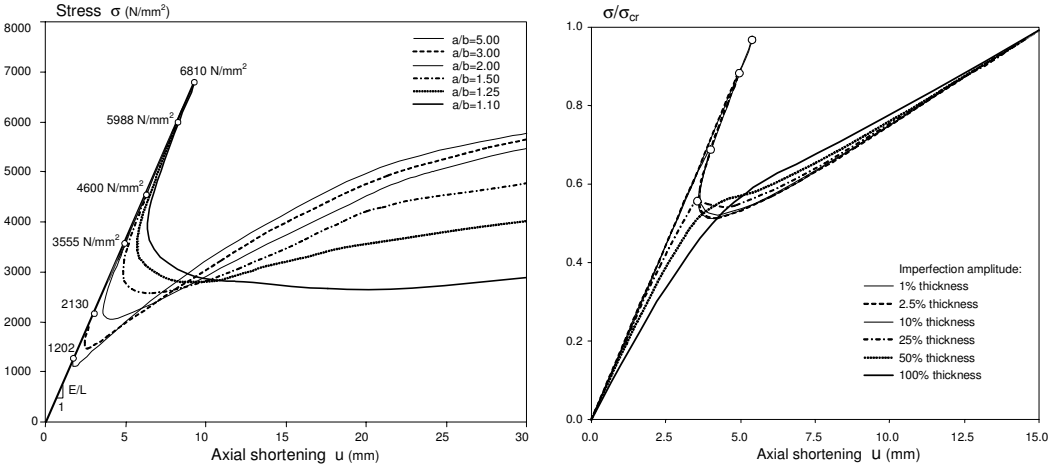

Figure 3: (a) Applied stress σ vs. axial shortening u for several a/b ratios (imperfection = 2.5% thickness) and (b) critical stress ratio σ/σ_{cr} vs. axial shortening u for a range of imperfections (a/b=2).

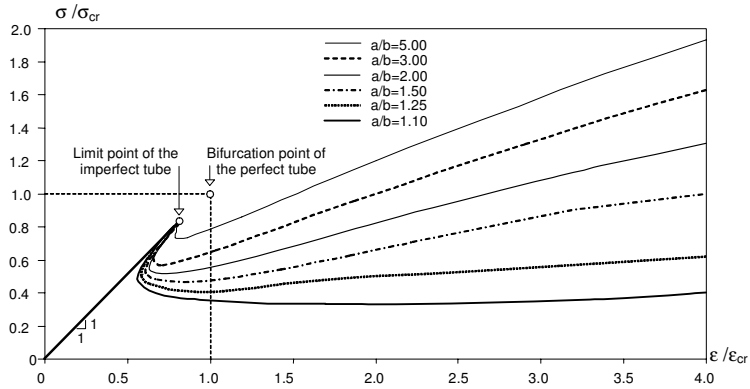

Figure 4: Relationship between the critical stress (σ/σ_{cr}) and strain ($\varepsilon/\varepsilon_{cr}$) ratio for varying a/b.

From careful observation of figures 3(a) and 4 the following comments can be made:

(i) The six tubes possess an equal cross-section area and, therefore, the slope of the primary path is given by E/L and is equal for all six tubes; the primary paths are also perfectly linear until the limit stress σ_{lim} is reached. As expected, the limit stress σ_{lim} is lower than the corresponding critical stress σ_{cr} due to the influence of the imperfections. The variation of limit stress σ_{lim} with aspect ratio is shown in table 1. In fact, the ratio between the limit stress and the critical stress (σ_{lim}/σ_{cr}) shows little variation with a/b and remains around 0.85 for the adopted imperfection amplitude of 2.5% of the EHS thickness. This suggests that the imperfection sensitivity of EHS tubes is not strongly dependent on the aspect ratio a/b of the cross-section, within the examined range of $1.10 < a/b < 5.00$.

(ii) After reaching the limit stress σ_{lim}, the six non-linear paths show very distinct responses. The descending branch (decrease of both applied stress and axial shortening) is much more pronounced for tubes with lower aspect ratio a/b, as shown in the graph of σ/σ_{cr} versus $\varepsilon/\varepsilon_{cr}$ given in figure 4.

(iii) Figure 3(a) shows that all the tubes are associated with post-critical curves that possess local minima, which move horizontally towards the linear primary path as the aspect ratio increases. Beyond the local minima the post-buckling paths (for $a/b \geq 1.10$) exhibit a positive slope (increase in applied stress and axial shortening) and are stable. It may be observed that the maximum slope of the ascending post-buckling branch increases with aspect ratio a/b, this increase being more substantial for low to moderate aspect ratios ($a/b \leq 2$) and less pronounced for moderate to high aspect ratio ($a/b \geq 2$). Furthermore, the slope of the ascending post-buckling path can reach values up to 40% of the initial slope of the linear primary path; a value similar to that for flat simply-supported plates with unrestrained edges.

(iv) From points (i) to (iii), it may be concluded that the maximum applied stress σ_{max} that an elastic EHS tube with low to moderate aspect ratio ($a/b \leq 1.5$) can support is its limit stress σ_{lim} whereas, the maximum applied stress σ_{max} that an elastic EHS tube with moderate to high aspect ratio ($a/b \geq 2.0$) can carry is higher than its limit stress σ_{lim} (see figure 3(a)). The initially unstable post-buckling response exhibited by all six tubes investigated (with an imperfection of 2.5% of the section thickness), means that snap-through behaviour is experienced at the limit stress. However, figure 3(a) shows that the snap-through reduces with increasing aspect ratio a/b. For instance, the very eccentric tube with a/b = 5.0 experiences, at the limit stress level σ_{lim}=1202 N/mm^2, a very small snap between u = 1.86 mm and u = 2.22 mm. Conversely, the moderately eccentric tube with a/b = 2.0 experiences, at the limit stress level σ_{lim}=3555 N/mm^2, a larger snap between u = 4.98 mm and u = 12.85 mm.

The deformed configurations of the EHS tubes in the post-buckling regimes are shown in figure 5, where deformation may be seen to be concentrated towards the mid-height of the specimens. Initial geometrical imperfections were imposed with an inward deformation of the flatter region (i.e. maximum local radius of curvature) of the EHS at mid-height (see figure 2). From figure 5, it may be seen that the

post-buckling deformed configurations are characterised by a pronounced flattening of the cross-section at its mid-height; this flattening is associated with high tensile normal stresses that develop in the transverse (circumferential) direction.

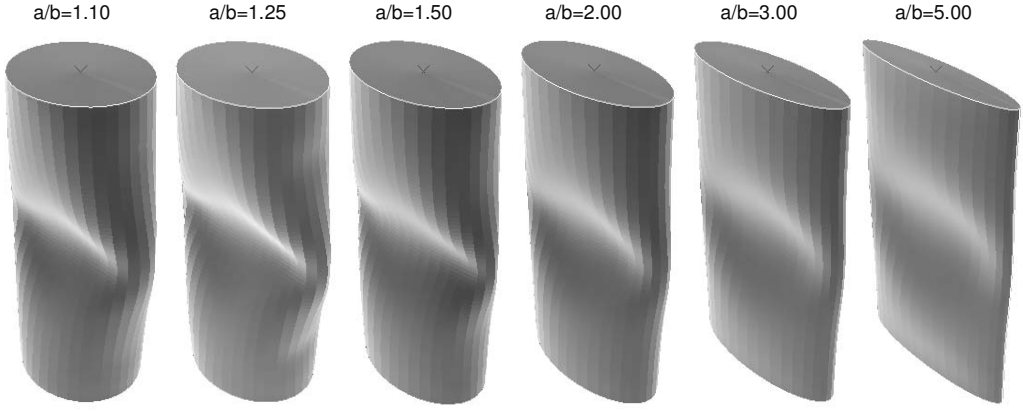

Fig. 5: Deformed configurations of the EHS tubes in the post-buckling regime.

5 NORMAL STRESS DISTRIBUTIONS

In order to explain the distinct post-critical behaviour exhibited by EHS tubes and its dependency on the aspect ratio a/b, the normal stress distributions in the weakest (most deformed) zone of the tube, (i.e., at mid height) are examined. Figure 6 comprises six graphs (for the six different aspect ratios investigated), each one showing the evolution of normal stress distributions $\sigma(\theta)$ for several load levels (σ/σ_{cr}), i.e., for several points travelling along the equilibrium path. In the key to each figure, the values of σ/σ_{cr} initially increase up to the limit stress, after which they decrease to the local minimum and then increase again; compressive stresses are positive. The normal stress $\sigma(\theta)$ is measured along the mid-line of the EHS and associated with membrane behaviour and θ is the angle to the centre of the EHS; (θ=0° and180° correspond to the points of minimum radius of curvature $r_{min} = b^2/a$, coincident with the EHS major axis, and θ=90° and 270° correspond to the points of maximum radius of curvature $r_{max} = a^2/b$, coincident with the EHS minor axis). The solid curves correspond to the limit stress ratio σ_{lim}/σ_{cr}. To aid comparison between the six diagrams, the normal stress $\sigma(\theta)$ axes have the same vertical scale. From observation of figure 6 the following remarks can be made:

(i) For $\sigma < \sigma_{lim}$ and independently of the aspect ratio a/b, the normal stress is essentially uniform along the EHS mid-line (i.e. σ is almost independent of θ). Further, as also seen in table 1, the stress level corresponding to $\sigma = \sigma_{lim}$ decreases with increasing aspect ratio a/b. From this observation, it could be interpreted that it is preferable to design EHS with lower aspect ratios – the CHS being the limit configuration. However, as will be seen later, such an approach does not truly corresponds to optimum EHS design.

(ii) For $\sigma > \sigma_{lim}$ and independently of the aspect ratio a/b, the normal stress ceases to remain uniform along the EHS mid-line (i.e. σ varies with θ). However, it should be highlighted that the non-linear distribution of $\sigma(\theta)$ varies markedly with aspect ratio a/b. The zones of maximum EHS radius of curvature (θ = 90° and 270°) are always in compression ($\sigma(\theta) > 0$) but the normal stress decreases continuously for increasing applied stress ratio (σ/σ_{cr}). The points of minimum EHS radius of curvature (θ = 0° and 180°) may be in compression or in tension, and this fact has far reaching implications for the stability of the post-buckling branches. Immediately after the peak (σ_{lim}), the normal stress in the θ=0° and 180° regions decreases for all a/b values; this decrease being much more pronounced for moderate to low aspect ratios (a/b ≤ 1.5) than for moderate to high aspect ratios (a/b ≥ 2.0).

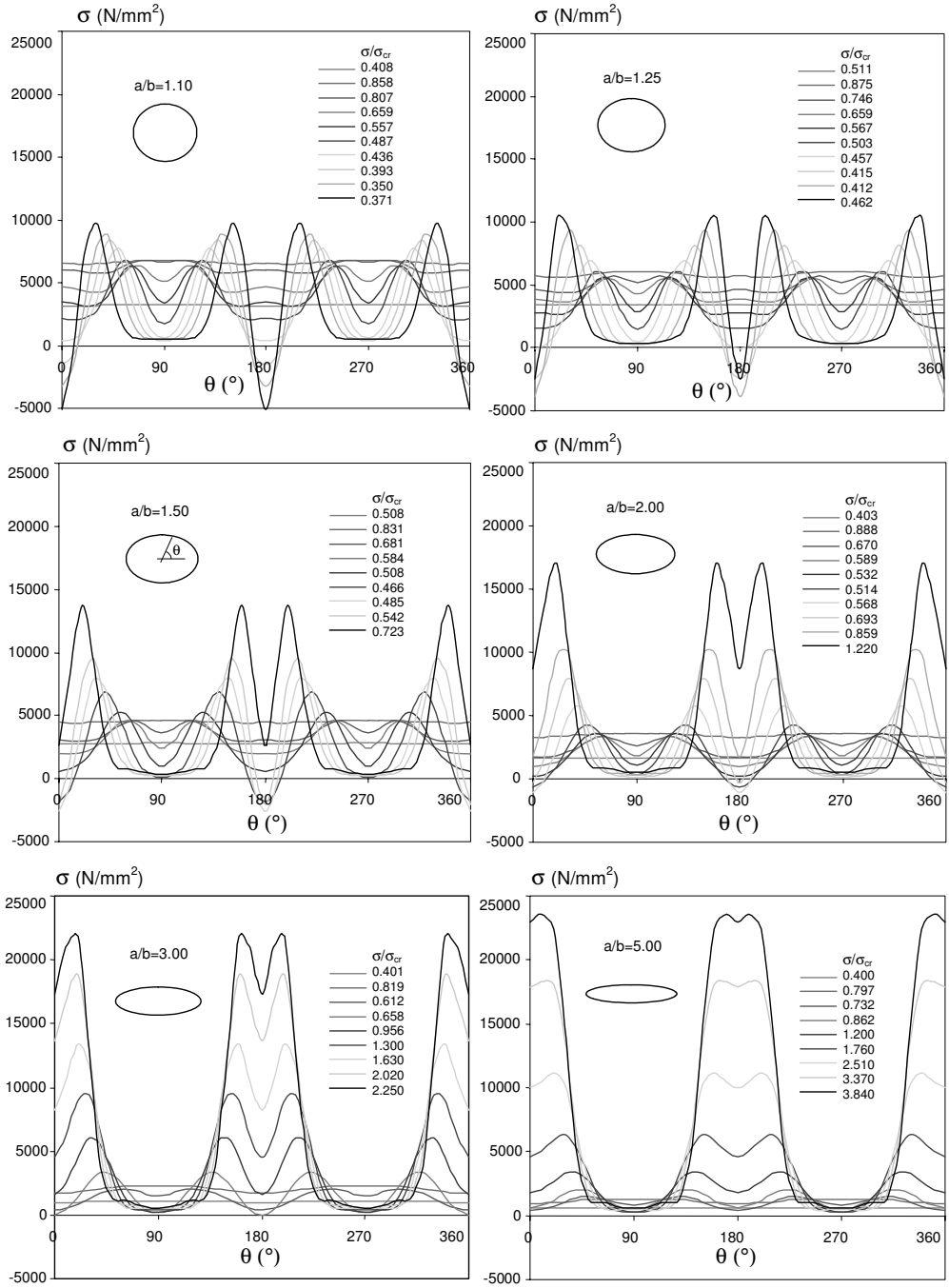

Figure 6: Evolution of normal stresses $\sigma(\theta)$ with σ/σ_{cr} for the six different aspect ratios a/b.

For a/b = 1.10, the stress decreases and changes sign, with the points of minimum EHS radius of curvature ($\theta = 0°$ and 180°) being in tension at the maximum axial shortening (black line). For $1.25 \leq a/b \leq 2.0$, the stress decreases and changes sign, but then tends to increase again with increasing displacement. For $3.0 \leq a/b \leq 5.0$, the stress slightly decreases after the peak but then increases significantly, and the points $\theta = 0°$ and 180° are never in tension. The points of maximum compressive stress are not at the minimum EHS radius of curvature ($\theta = 0°$, 180°) but are immediately adjacent to these points at θ = 10-30°, 150-170°, 190-210° and 330-350°.

(iii) As noted above, non-linear distributions of $\sigma(\theta)$ vary markedly with aspect ratio a/b. For low to moderate aspect ratios ($a/b \leq 1.5$), the stress distribution in the zones of minimum EHS radius of curvature ($\theta < 60°$, $120° < \theta < 240°$, $\theta > 300°$) is distinctly non-linear with θ, with compressive and tensile stresses occurring over different ranges of θ. For increasing aspect ratio ($a/b \geq 1.5$), the stress distribution in the zones of minimum EHS radius of curvature ($\theta < 60°$, $120° < \theta < 240°$, $\theta > 300°$) becomes more uniform. This may be seen most clearly for the EHS tube with a/b = 5, where the compressive stresses are almost uniform inside the ranges $\theta < 60°$, $120° < \theta < 240°$ and $\theta > 300°$, for the maximum axial shortening (black line).

(iv) For EHS tubes with low aspect ratio a/b, the development of tension stresses in the zones of minimum EHS radius of curvature lead to a "softening effect" in behaviour of the tube, since the average stress along the EHS mid-line reduces as the tensile stresses grow. This is the reason for the almost horizontal post-buckling branches following the initial drop in load (see figure 3(a)) exhibited by the EHS tubes with a/b = 1.1 and 1.25; their post-buckling behaviour is similar to that exhibited by circular shells and they do not possess any post-critical stiffness. Conversely, for EHS tubes with moderate to high eccentricity (or aspect ratio a/b), the development of high compressive stresses in the zones of minimum EHS radius of curvature lead to a "hardening effect" in behaviour of the tube, since the average stress along the EHS mid-line now tends to increase as the compressive stresses grow. This is the reason for the ascending and stable post-buckling branches (see figure 3(a)) exhibited by the of EHS tube with a/b = 1.5, 2.0, 3.0 and 5.0. Consequently, their post-buckling behaviour is closer to that exhibited by flat plates and they do possess notable post-critical stiffness.

(v) On the basis of the above findings, it may be concluded that an approach based on the "effective width concept", widely used for the strength analysis of flat plates, may be adapted to the design of EHS tubes with moderate to high aspect ratios. This procedure is outside of the scope of the present paper, but is the subject of ongoing research.

6 IMPERFECTION SENSITIVITY

In previous sections, a constant imperfection amplitude of 2.5% of the section thickness has been adopted. In this section, the imperfection sensitivity of EHS tubes under compression is examined. Each of the six tubes was analysed for six imperfection amplitudes: ξ = 0.04 mm (1% of the thickness), ξ = 0.10 mm (2.5% of the thickness), ξ = 0.4 mm (10% of the thickness), ξ = 1.0 mm (25% of the thickness), ξ = 2.0 mm (50% of the thickness) and ξ = 4.0 mm (100% of the thickness). For the tube with a/b = 2, figure 3(b) shows the equilibrium paths (critical stress ratio σ/σ_{cr} versus axial shortening u) obtained for the several imperfection amplitudes. It is clear that, for imperfection amplitudes lower than 25% of the thickness, the equilibrium paths possess a limit point, and the limit stress σ_{lim} decreases significantly with increasing imperfection amplitude. Conversely, for imperfection amplitudes higher than 50% of the tube thickness, (i) the equilibrium paths always ascend and (ii) there is no limit stress. This behavioural aspect has far reaching implications for the imperfection sensitivity of EHS tubes: due to its stable and ascending post-buckling branch, a moderately (or highly) eccentric EHS tube may or may not be imperfection sensitive depending on the range of imperfections being considered. For a given aspect ratio a/b, there is always a "bound imperfection amplitude" (ξ_b) that separates the ranges of imperfection amplitude where the tube is imperfection sensitive ($\xi < \xi_b$) and insensitive ($\xi > \xi_b$). From figure 3(b), for the EHS tube with a/b = 2, this ξ_b value should lie between 25% and 50% of the thickness. Using a trial-and-error procedure, the exact value of the "bound imperfection amplitude" was found to be ξ_b = 1.2mm = 30% of the thickness.

7 CONCLUSIONS

The elastic local post-buckling behaviour of tubes with elliptical hollow sections (EHS) under compression was analysed in this paper. The obtained numerical results were then presented and analysed; the following conclusions are drawn:

(i) Non-linear equilibrium paths - The maximum applied stress that an elastic EHS tube with low to moderate aspect ratio ($a/b \leq 1.5$) can support is its limit stress σ_{lim}, while the maximum applied stress that an elastic EHS tube with moderate to high aspect ratio ($a/b \geq 2.0$) can carry is higher than its limit stress σ_{lim}. It was observed that the slope of the ascending branch increases with aspect ratio a/b and can reach values up to 40% of the initial slope of the linear primary path.

(ii) Normal stress distributions - For increasing aspect ratio a/b, the compressive stresses grow and accumulate near the zones of minimum radius of curvature while the zones of maximum radius of curvature possess an approximately uniform and relatively low compressive stress level. Therefore, it is expected that an approach based on the "effective width concept" widely used for the strength analysis of flat plates may be adapted to the design of EHS tubes with moderate to high aspect ratios.

(iii) Imperfection sensitivity - For a given aspect ratio a/b, there is a "bound imperfection amplitude" ξ_b that separates the ranges of imperfection amplitude where the EHS tube is imperfection sensitive ($\xi < \xi_b$) and insensitive ($\xi > \xi_b$). Moreover, it was shown that the imperfection sensitivity of EHS tubes significantly drops for increasing aspect ratio a/b, ranging between shell-type behaviour (strongly imperfection sensitive) and plate-type behaviour (imperfection insensitive).

REFERENCES

[1] Corus. Celsius 355s Ovals. Internet: http://www.corusgroup.com, 2006.

[2] Interpipe – The Hollow Section Company. Elliptical Hollow Sections to S355 J2H, Internet: http://www.interpipe.co.uk/, 2007.

[3] CEN – Comité Européen de Normalisation. *EN 10210-2: Hot finished structural hollow sections of non-alloy and fine grain steels – Part 2: Tolerances, dimensions and sectional properties*, 2006.

[4] Gardner, L., Chan, T.M., "Cross-section classification of elliptical hollow sections", *Steel and Composite Structures*, **7**(3), 185-200, 2007.

[5] Chan, T.M., Gardner, L., "Compressive resistance of hot-rolled elliptical hollow sections", *Engineering Structures*, **30**(2), 522-532, 2008.

[6] Chan, T.M., Gardner, L., "Flexural buckling of elliptical hollow section columns", *Journal of Structural Engineering-ASCE*, **135**(5), 546-557, 2009.

[7] Zhu, Y., Wilkinson, T., "Finite element analysis of structural steel elliptical hollow sections in compression", *Research Report No R874*, Centre for Advanced Structural Engineering, The University of Sydney, 2007.

[8] Silvestre, N., "Buckling behaviour of elliptical cylindrical shells and tubes under compression", *International Journal of Solids and Structures*, **45**(16), 4427-4447, 2008.

[9] Ruiz-Teran, A.M., Gardner, L., "Elastic buckling of elliptical tubes", *Thin-Walled Structures*, **46**(11), 1304-1318, 2008.

[10] DS Simulia Inc. *ABAQUS Standard* (version 6.7), 2007.